



# In-depth characterization of a cysteine-linked ADC disitamab vedotin by multiple LC-MS analysis methods and cutting-edge imaged capillary isoelectric focusing coupled with native mass spectrometry

Gang Wu<sup>a,1</sup>, Xiaoxi Zhang<sup>b,1</sup>, Xin Wang<sup>c</sup>, Jialiang Du<sup>a</sup>, Meng Li<sup>a</sup>, Gangling Xu<sup>a</sup>, Min Du<sup>d</sup>, Chuanfei Yu<sup>a,\*</sup>

<sup>a</sup> National Institutes for Food and Drug Control, State Key Laboratory of Drug Regulatory Science, NHC Key Laboratory of Research on Quality and Standardization of Biotech Products, NMPA Key Laboratory for Quality Research and Evaluation of Biological Products, Daxing District, Beijing, 102629, China

<sup>b</sup> Thermo Fisher Scientific, Shanghai, 200000, China

<sup>c</sup> Fujian Institute for Food and Drug Quality Control, Fuzhou, 350000, China

<sup>d</sup> Thermo Fisher Scientific, Lexington, MA, 02421, US

## ARTICLE INFO

### Keywords:

Imaged capillary isoelectric focusing  
Mass spectrometry  
Strong cation exchange chromatography  
Antibody-drug conjugates  
Charge heterogeneity

## ABSTRACT

The characterization of cysteine-linked antibody–drug conjugates (ADCs) can be more challenging than that of monoclonal antibodies (mAbs) and lysine-linked ADCs because the interchain disulfide bonds are reduced for payload conjugation, and the chains are noncovalently bonded to each other. Furthermore, payload conjugation and disulfide bond reduction/scrambling may introduce additional charge heterogeneity to biomolecules. This study illustrates an innovative workflow employing multiple separation techniques and tandem high-resolution mass spectrometry for comprehensive and in-depth characterization of disitamab vedotin, a recent-generation cysteine-linked ADC, including reversed-phase liquid chromatography (RPLC), ion exchange chromatography (IEX) and image capillary isoelectric focusing (icIEF). RPLC was employed for reduced chains analysis, subunit analysis and peptide mapping. IEX and icIEF were used for charge heterogeneity analysis. The innovation of the integrated methodology emphasizes the importance of cutting-edge icIEF-MS online coupling under near-native conditions to reveal the heterogeneity of disitamab vedotin.

## 1. Introduction

Antibody-drug conjugates (ADCs) are at the forefront of the next generation of biopharmaceuticals. ADC is typically composed of an antibody covalently attached to a cytotoxic drug via either a permanent or a labile linker, creating a highly heterogeneous product [1]. One of the pioneering first-generation ADCs, gemtuzumab ozogamicin, was approved by FDA in 2000 under the trade name Mylotarg® [2] but was withdrawn from the market in June 2010 due to a significantly higher fatal toxicity rate [3], and it was reapproved by FDA in 2017 based on new clinical data. Brentuximab vedotin and Ado-trastuzumab emtansine are two representatives of second-generation ADCs [4,5]. Compared to first-generation ADCs, second-generation ADCs show good clinical efficacy and safety [4–7]. However, they still have shortcomings, such as DAR distributions, and ADCs with DARs greater than 4 have lower

tolerability and efficacy and greater plasma clearance. The cytotoxins employed in second-generation ADCs do not have very specific targets; therefore, serious adverse reactions such as liver toxicity may occur, resulting in a very narrow therapeutic window. Additionally, these ADCs have limited cell penetration ability, which also affects their efficacy and can cause side effects [8–10]. The intensive approval of third-generation ADCs (represented by polatuzumab vedotin, under the trade name Polivy®) marked an explosive period for ADCs. Third-generation ADCs combine factors that fail the first and second generations. With more site-specific payload conjugation technology, third-generation ADCs have reduced toxicity and fewer naked monoclonal antibodies, and their stability and pharmacokinetics have also greatly improved [11].

The ADC used in this study, disitamab vedotin, sold under the trade name Aidixi®, is a cysteine-linked ADC comprising a monoclonal antibody against human epidermal growth factor receptor 2 (HER2)

\* Corresponding author.

E-mail address: [yucf@nifdc.org.cn](mailto:yucf@nifdc.org.cn) (C. Yu).

<sup>1</sup> The authors contributed equally to this article.

<https://doi.org/10.1016/j.chroma.2024.465353>

Received 5 July 2024; Received in revised form 4 September 2024; Accepted 6 September 2024

Available online 8 September 2024

0021-9673/© 2024 Elsevier B.V. All rights are reserved, including those for text and data mining, AI training, and similar technologies.

conjugated via a cleavable linker to the cytotoxic agent MMAE [12]. In June 2021, disitamab vedotin received its first Biologics License Application (BLA) approval in China for the treatment of patients with HER2-overexpressing (defined as IHC2+ or 3+) locally advanced or metastatic gastric cancer (including gastroesophageal junction adenocarcinoma) who have received at least two systemic chemotherapy regimens [12,13]. The design of disitamab vedotin enables targeted delivery of cytotoxic drugs to neoplastic cells, reducing systemic toxicity [11-14].

Due to the extreme complexity of ADCs in the presence of antibodies, linkers and payloads, a single analytical platform cannot achieve accurate characterization of such complex heterogeneities. Employing a portfolio containing comprehensive technologies is essential for addressing CQAs, which may affect product safety and drug efficacy [15, 16]. A recent publication reviewed the analytical strategies for complex protein characterization, including mass spectrometry and chromatography [17]. UHPLC, both one dimension and two dimensions separation, HRMS/MS and IEX-MS have been widely utilized for in-depth characterization of complex protein drugs [18-21].

IEX, a traditional chromatographic technique, and icIEF, a standard electromigration technique in the biopharma industry, are the most important front-end separation techniques for MS-based charge variant analysis of proteins; however, IEX and icIEF have different separation mechanisms. Kaur et al. indicated that "IEX, unlike cIEF/icIEF, does not separate analytes based on overall charge, but on the charge available for interaction with the solid phase. Thus, a particular proteoform could be separated by capillary electrophoresis but not by IEX, thereby yielding complementary information as orthogonal techniques" [22]. Füssl et al. had reported the combination of cation exchange chromatography and capillary electrophoresis coupled to mass spectrometry for mAb charge heterogeneity characterization [23], Wu compared the IEX-MS and icIEF-MS results of nine therapeutic mAbs [24]. Both studies proved the necessity of employing orthogonal separation techniques for charge variant analysis. icIEF has become an indispensable tool in therapeutic protein development and manufacturing because of its high analytical throughput, ease of use, fast method development and excellent reproducibility [25]. icIEF is a robust tool for characterizing the heterogeneity of ADCs [25-29]. Recently, icIEF-MS has attracted much attention for its use in protein charge variant analysis, including microfluidic chip-based and capillary-based icIEF-MS for mAbs and bispecific antibodies [30-37]. However, icIEF-MS for cysteine-linked ADCs is still challenging because intact MS for cysteine-linked ADCs requires native condition and the parameters need to be systematically optimized. Xu et al. [38] reported native cIEF-MS methods for characterize intact protein complexes but only intact level studies were performed, and individual fractions were not collected for further characterization.

In this study, a MS-based workflow integrating comprehensive separation techniques was developed to characterize the complex heterogeneity of disitamab vedotin. Native intact MS, reduced chain and subunit analysis under denaturing condition and peptide mapping were utilized for in-depth characterization of this molecule. Online SCX-UV-MS was applied to fingerprint the charge heterogeneity of the ADC, and the results were consistently verified by native intact MS and peptide mapping of SCX offline fractionations. Online cutting-edge icIEF-MS coupling under near-native condition was applied for charge variant analysis, and the combination of online SCX-UV-MS and icIEF-MS are complementary techniques for charge heterogeneity analysis. The established workflow was a comprehensive and innovatively integrated multiple separation technique coupled with high-resolution MS for cysteine-linked ADC characterization. In addition, this is the first time that disitamab vedotin has been fully characterized using a UHPLC-HRMS platform.

## 2. Materials and methods

### 2.1. Chemicals

The disitamab vedotin studied in this work was retained sample from the author's organization (National Institutes for Food and Drug Control). Mass spectrometry grade water, acetonitrile (ACN), CX-1 pH gradient buffers, formic acid, acetic acid, Tris-HCl, ammonium bicarbonate and ammonia were purchased from Fisher Scientific. Guanidine hydrochloride, sodium iodoacetate, DL-dithiothreitol and ammonium acetate were purchased from Sigma-Aldrich. Trypsin and IdeS enzymes were purchased from Promega. All the ampholytes (AESlytes) were obtained from Advanced Electrophoresis Solutions Ltd. (AES, Cambridge, Ontario, Canada).

### 2.2. Sample preparation

For icIEF-MS sample preparation, the sample was loaded onto a spin column insert tube and then centrifuged 3 times at  $21,000 \times g$  for 10 min, 200  $\mu$ l of ddH<sub>2</sub>O was loaded each time for buffer exchange; ddH<sub>2</sub>O was used to adjust the final protein concentration to 2 mg/mL with 1 % HR3-10 and 1 % HR8.5-9.5 carrier ampholytes.

Sample preparation for native intact MS, SCX-UV-MS, reduced chain, subunit analysis and peptide mapping can be found in the Supporting Information.

### 2.3. Parameters for SCX-UV-MS

For SCX-UV-MS separation, a Vanquish UHPLC system was used with mobile phases composed of relative combinations of A (25 mM ammonium bicarbonate and 10 mM acetic acid, pH 5.3) and B (10 mM ammonia, pH=10.9). A Thermo Scientific™ ProPac™ 3R SCX 3  $\mu$ m HPLC column (2  $\times$  50 mm, P/N 43103-052068) was used. A total of 40  $\mu$ g of sample was loaded onto the column, the flow rate was 0.3 mL/min, and the column temperature was 40 °C. The gradient elution programs were 0-2 min, 0 % B, 2-30 min, 5-100 % B, 30-32 min, 100 % B, 32-41 min, 0 % B. A Thermo™ Scientific™ Orbitrap™ Exploris™ 240 Mass Spectrometer equipped with Biopharma option was used for mass measurements. MS settings: spray voltage 3.6 kV, sheath gas 35 Arb, auxiliary gas 10 Arb, S-lens RF 200, capillary temperature 250 °C, vaporizer temperature 200 °C, resolution 60,000@ $m/z$  200, scan range of precursor ion 2500-8000  $m/z$ , source fragmentation 120 eV, intact protein mode (high pressure).

### 2.4. Parameters for icIEF-MS under near-native condition

For icIEF separation, the CEInfinite icIEF system (Advanced Electrophoresis Solutions Ltd., Cambridge, Canada) was utilized with on-column UV detection at 280 nm. 200  $\mu$ m ID acrylamide derivative (AD)-coated capillary cartridges with microtee integration (AES, cat. no. CP00303M) were used for icIEF-MS. The length of separation capillary is 5 cm and sample loading volume is about 1.6  $\mu$ L. The catholyte and anolyte used in this study were purchased from Advanced Electrophoresis Solutions Ltd. (AES, cat. no. 101,010). In icIEF analysis, focusing was performed at 1 min-1000 V, 1 min-2000 V and 10 min-3000 V. 3000 V was applied during the pressure driven mobilization of focused protein bands; the mobilization speed was 70 nL/min with 0.1 % formic acid, H<sub>2</sub>O and 3  $\mu$ L/min make-up solution (10 mM NH<sub>4</sub>Ac:ACN=9:1). The mobilization time was 50 min. An Orbitrap Exploris 240 Mass Spectrometer equipped with Biopharma option and an assembled low-flow ESI metal needle (34-gauge) was used for mass measurements. MS settings: spray voltage, 3.8 kV; sheath gas, 0 Arb; auxiliary gas, 4Arb; S-lens RF, 200; capillary temperature, 250 °C; vaporizer temperature, 40 °C; resolution, 60,000@ $m/z$ , 200; scan range of precursor ions, 2500-8000  $m/z$ ; source fragmentation, 120 eV; and intact protein mode (high pressure).

The parameters for native intact MS, reduced chains, subunit analysis and peptide mapping can be found in the Supporting Information.

Biopharma Finder™ software (version 5.1) from Thermo Fisher was used for data analysis.

### 3. Results and discussion

Fig. 1 illustrates a MS-based workflow integrating comprehensive chromatographic techniques for characterizing cysteine-linked ADC heterogeneity. The obtained results can be compared and cross-validated for more comprehensive and accurate insights into the complexity of cysteine-linked ADC heterogeneity.

#### 3.1. Native intact MS, reduced chains and subunit analysis of disitamab vedotin

The maleimidocaproyl-valinecitruilline-p-aminobenzyloxycarbonyl linker monomethyl auristatin E (MC-vc-PAB-MMAE) is used for bioconjugation in disitamab vedotin [12–14]. The mAb is partially reduced for conjugation, which leads to a payload distribution of 0, 2, 4, 6 or 8. This cleavable heterobifunctional maleimide linker facilitates the release of MMAE after internalization in target tumor cells [11]. The cytotoxin MMAE inhibits cell division by disrupting tubulin polymerization [6] and cannot be used as a standalone drug due to its inherent toxicity. Therefore, the DAR value becomes critically important when MMAE is used as an ADC payload. As reported, the average DAR of disitamab vedotin is approximately 4 [12,13]. Figure S1 in the Supporting Information presents a schematic diagram of all the theoretical conjugation forms of disitamab vedotin (D0 to D8). Since interchain disulphide bonds are reduced for conjugation, native intact MS has been a routine technique for cysteine-linked ADC MW and DAR measurements because the non-covalent interactions between chains can be maintained under native condition [39].

Fig. 2 displays the native intact MS spectra and deconvolution results of disitamab vedotin. As described above, linker-drug conjugation results in high structural heterogeneity. In the zoomed-in view of the  $m/z$

range of 5300–5600 Da (bottom row), it is easy to notice that the distributions have very close  $m/z$  values, and the same situation is observed for D2 ( $z=+27$ ) and D6 ( $z=+28$ ). The study demonstrated that the high resolution and sensitivity provided by the Orbitrap mass analyzer enabled the separation and identification of peaks in such complex samples, leading to precise, intact MS measurement results. The deconvolution results of disitamab vedotin in Fig. 2 demonstrate the successful identification of the major N-glycans from D0 to D8. From D2 to D8 a consistent distribution of the major N-glycans, such as  $2 \times A2G0F$ ,  $A2G0F+A2G1F$  and  $2 \times A2G1F$ , etc. were identified. These results were in agreement with reduced chains analysis, subunit analysis and peptide mapping results in following section and supporting information 4 and 5. Notably, odd-numbered payload isoforms such as D3, D5, and D7 were detected, although the payload numbers should theoretically be even. Most likely, these minor species arose from unexpected payload conjugation, demonstrating the benefits of the high resolution and sensitivity offered by the high-resolution MS platform. The average DAR value automatically calculated by BioPharma Finder software was 4.19, which aligns well with previous publications [12,13].

In the reduced chains analysis of disitamab vedotin, the remaining interchain disulphide bonds were broken after DTT treatment, which generated a mixture of LC D0 and D1 and HC D0 to D3. Figure S2A in the Supporting Information showed reduced chains analysis MS spectra under denaturing condition. Linker-drug payload conjugation introduced additional structural heterogeneity to both chains, and differences were observed at the full MS level. The MW of each LC/HC isoform is presented in the deconvolution results, as shown in Figure S2B and Table S1 in the Supporting Information, where glycation and succinimidation were detected. Additionally, an MC-vc-PAB-MMAE partially fragmented ( $-761.49$  Da) isoform [40] of LC D1 was detected. Both the linker-drug payload and glycosylation distributions of HC were identified.

For the subunit analysis of disitamab vedotin, IdeS enzyme digestion followed by DTT reduction was applied, yielding the three subunits Fc, LC and Fab. Subunits carrying different payloads (LC D0 and D1, Fab D0 to D3) and exhibiting N-glycosylation (Fc) were chromatographically

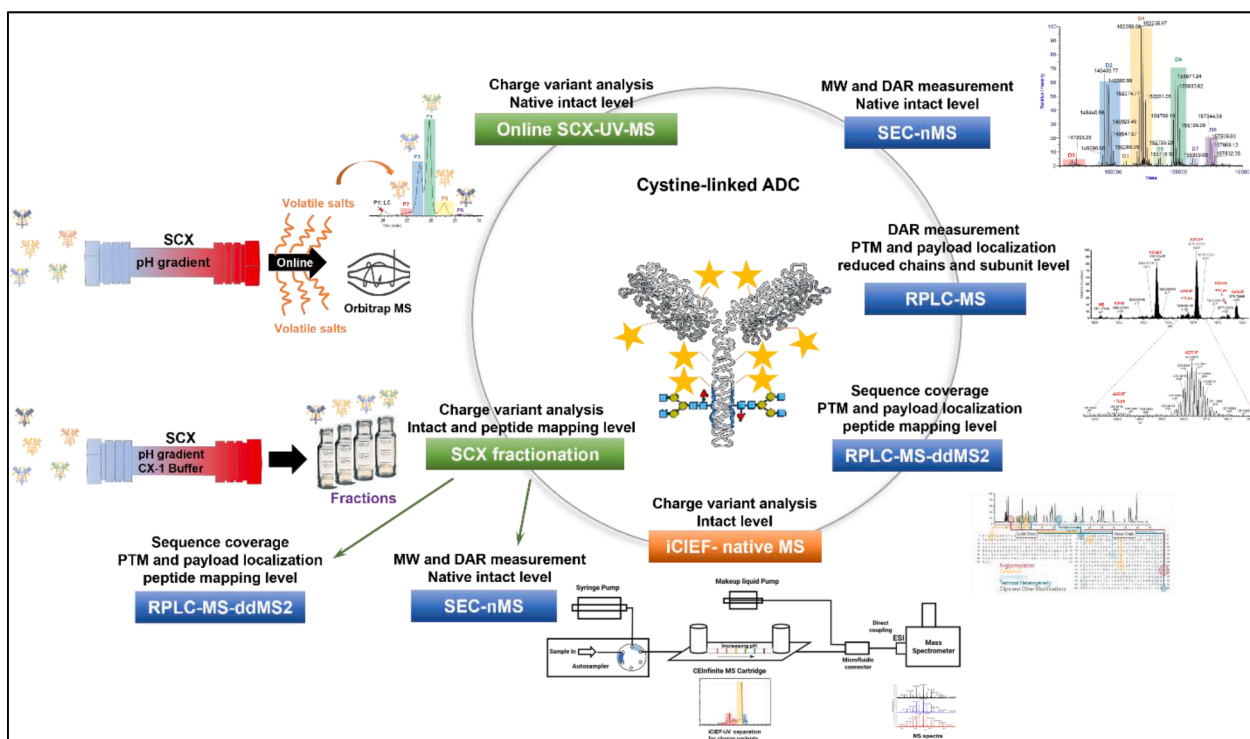


Fig. 1. Characterization workflow of cysteine-linked ADC heterogeneity.

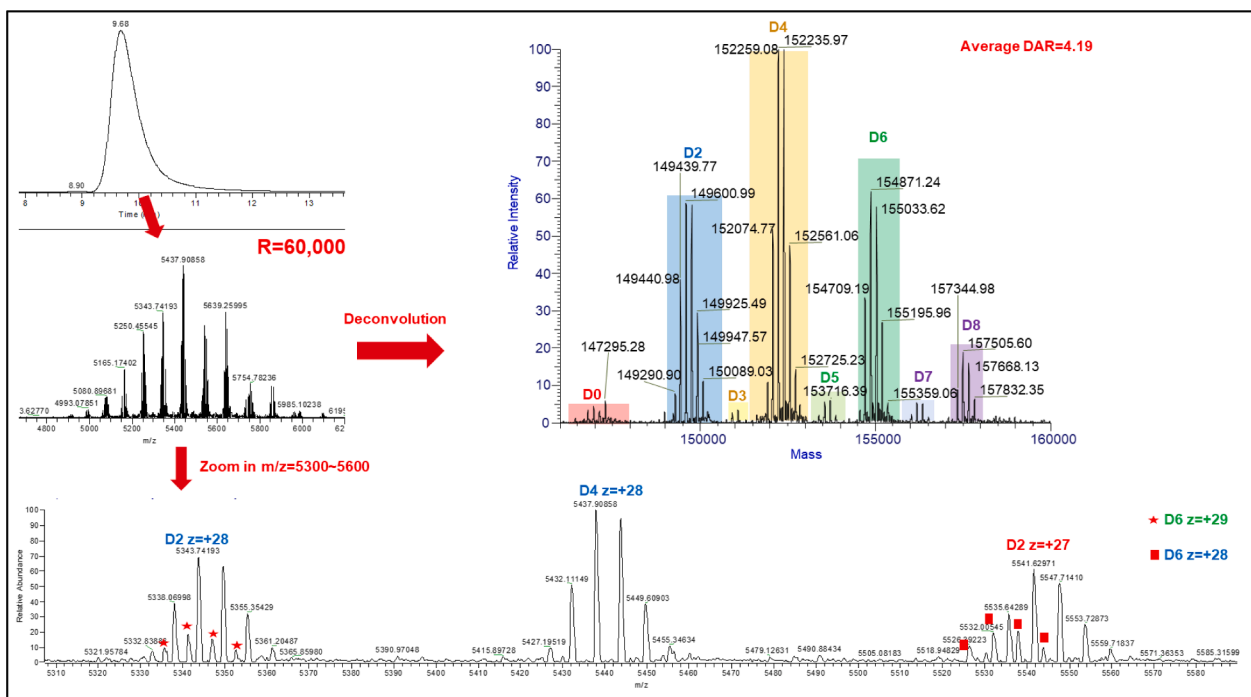


Fig. 2. Native intact MS and deconvolution result of disitamab vedotin.

separated and successfully identified (Figure S2C). The application of a higher resolution setting of 240,000 in subunit analysis resulted in baseline isotopically resolved spectra (Figure S2C zoom-in view) and the monoisotopic mass upon deconvolution (Figure S2D in the Supporting Information and Table S2), providing additional benefits for the characterization of complex biotherapeutics, such as ADCs, since modifications such as oxidation, succinimide and glycation can be detected at the subunit level. The deconvolution results in Figure S2D in the

Supporting Information and Table S2 provided abundant information, such as linker-drug payload distribution among LC/Fab isoforms, N-glycosylation and other modifications at subunits.

The reduced chains and subunit analysis of ADCs provided complementary information, including oxidation products, ADCs with varying payloads, and combinations of PTMs. It also has the advantages of straightforward sample preparation and data interpretation.

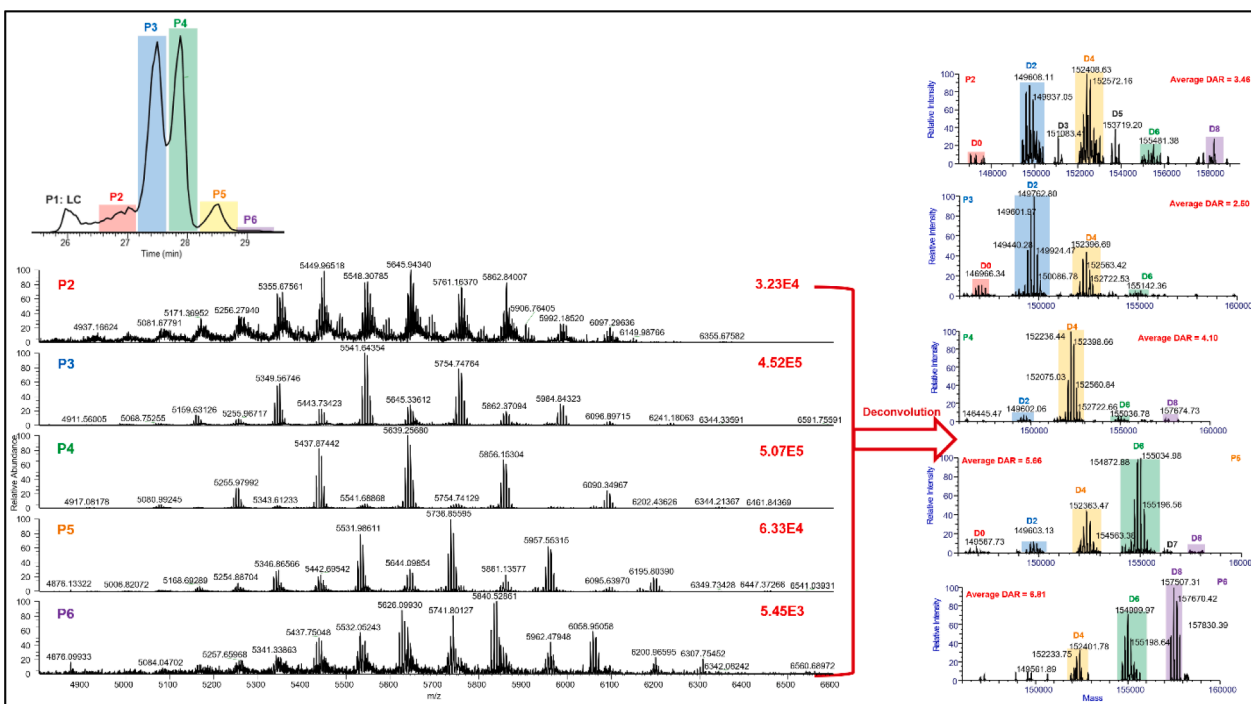


Fig. 3. SCX-MS analysis of disitamab vedotin. Upper left, BPC profiles of disitamab vedotin charge variant analysis using MS compatible buffer system. Lower left, the raw spectra of each peak from disitamab vedotin charge variant analysis. Peak 1 contains light chain fragments; intact ADC variants were detected from peak 2 to peak 6. Right, deconvolution result of each peak from disitamab vedotin charge variant analysis.

### 3.2. SCX-UV-MS of disitamab vedotin

PTMs such as deamidation, oxidation, succinimide, isomerization and lysine truncation can introduce charge heterogeneity to mAbs. For ADCs, payload conjugation can increase the charge heterogeneity of the biomolecule, as previously reported [40]. Therefore, separation techniques based on protein charge heterogeneity, such as capillary electrophoresis (CE) and SCX, have been used for the separation and identification of ADC charge variants [41,42]. We optimized the UHPLC parameters for ADC analysis based on the literature [24]. Fig. 3 showed the SCX-MS analysis results for disitamab vedotin. Using MS-compatible buffers, six peaks were separated and identified, including LC isoforms (peak 1) and intact ADC charge variants (peak 2 to peak 6). Fig. 3 also showed the raw spectra of peak 2 to peak 6 with different distributions (Fig. 3, lower left), which indicated the high charge heterogeneity of disitamab vedotin. High signal-to-noise (S/N) ratios and baseline separations of adjacent N-glycoforms were observed in all the spectra, and Fig. 3 (right column) showed the deconvolution results of each peak from the disitamab vedotin charge variant analysis. From peaks 2–6, as the pI increased, the number of payloads also increased. In peak 2, ADCs D0 to D8 were detected, but the percentages of D6 and D8 were much lower than those in the sample without SCX separation, while the percentages of D3 and D5 were greater. D2 was the most abundant type in peak 3, with D4 having a relative abundance of approximately 45%. D4 was the most abundant type in peak 4, while the relative abundances of D2 and D6 were lower than 10%. In peak 5, D6 was the most abundant isoform, and the second most abundant isoform was D4 at approximately 40%. In peak 6, D8 was the most abundant type, and D4 (approximately 30%) and D6 (approximately 70%) could still be detected.

SCX-UV-MS can separate different payload isoforms of disitamab vedotin based on charge heterogeneity, primarily through payload conjugation. The chromatographic peaks were not baseline separated, this result comes from secondary interactions between the ADC and the stationary phase mainly driven by the hydrophobic interactions with the hydrophobic drugs [43]. This approach can significantly reduce the complexity of subsequent online MS spectra and enhances confidence in the MW measurement results. It is a universal approach and requires little optimization for different biomolecules.

### 3.3. Peptide mapping of disitamab vedotin

Peptide mapping is a widely used characterization approach in the biopharmaceutical industry, providing detailed information about the molecule, including sequence coverage, PTM sites and percentages and disulphide bonds. In this study, disitamab vedotin was digested using trypsin, as described in the Supporting Information 1. The sequence coverage of HC was 94.8% and 97.2% for LC with MS/MS identification, respectively. The incomplete coverage was caused by the generation of short peptides two or three amino acids in length, which were too short for MS/MS identification. Combining results from multiple enzyme digestions can help to achieve 100% sequence coverage.

Peptide mapping can provide a thorough understanding of payload conjugation sites and other PTMs. Three peptides carrying four potential conjugation sites were identified: the hinge region peptide *THTC(224)PPC(227)PAPELLGGPSVFLFPPKPK* and the peptides *GEC(212)* and *SC(218)DK* generated from LC–HC interchain disulphide bond reduction. The payload conjugation increases the hydrophobicity of drug-loaded peptides [44] and can diminish MS signals. However, the exceptional sensitivity of the HRMS platform used in this study allowed for the collection of sufficient information on these peptides. Fig. 4 detailed the hinge-conjugated peptides, including the extracted ion chromatogram (XIC) peak, MS2 spectra, and fragment coverage map of all possible payload-conjugated isoforms. Notably, two possible payload-conjugated isoforms of this hinge region peptide, *THTC(224+MC-vc-PAB-MMAE)PPC(227+carboxymethylation)PAPELLGGPSVFLFPPKPK* and *THTC(224+carboxymethylation)PPC(227+MC-vc-PAB-MMAE)PAPELLGGPSVFLFPPKPK*, have identical MWs and highly similar peptide b/y ions. Their chromatographic behaviors differed, and several b/y ions contributed to confirming the conjugation sites. As shown in Fig. 4, the *THTC(224+MC-vc-PAB-MMAE)PPC(227+carboxymethylation)PAPELLGGPSVFLFPPKPK* isoform eluted earlier than the other isoform. For the peptides *GEC(MC-vc-PAB-MMAE)* and *SC(MC-vc-PAB-MMAE)DK*, peptide b/y ions were limited due to their short length. However, the peptide MW and characteristic fragmentation ions of MC-vc-PAB-MMAE [45] provided sufficient evidence for confirmation (Figure S3). Other PTMs, such as N-glycosylation, oxidation, deamidation, succinimide and aspartic acid isomerization, were presented in Figure S4 and Table S3 in the Supporting Information.

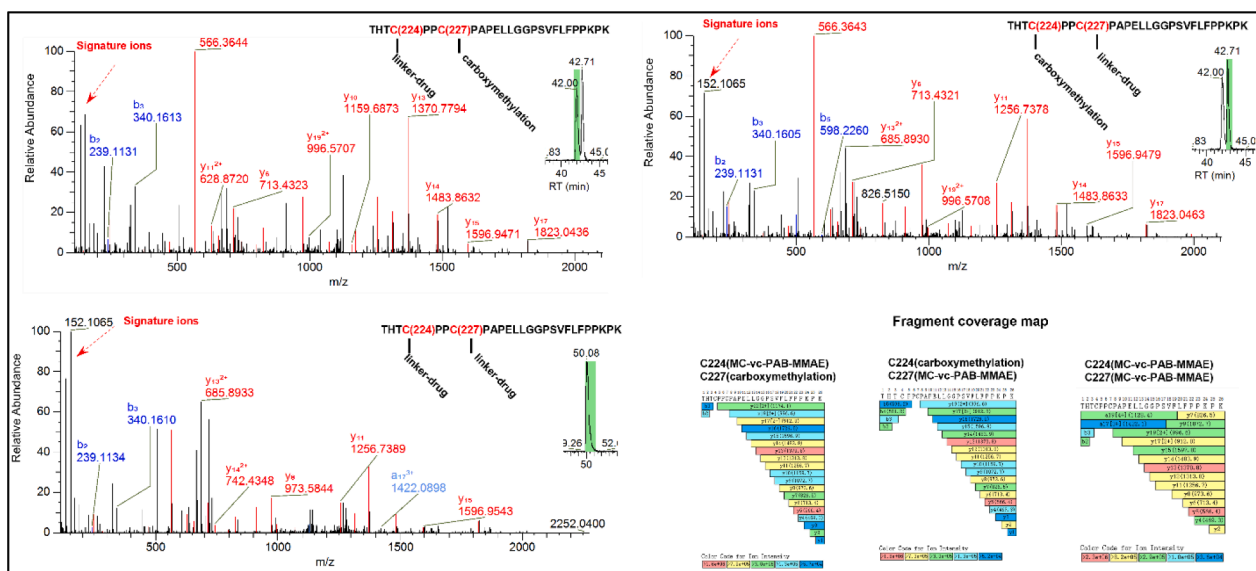


Fig. 4. The XIC peak and full MS and MS2 spectra of the hinge region peptide *THTC(224)PPC(227)PAPELLGGPSVFLFPPKPK* conjugated isoforms, signature fragmentation ions of MC-vc-PAB-MMAE are marked with red arrows.

### 3.4. SCX fractionation integrating native intact MS and peptide mapping for charge heterogeneity characterization of disitamab vedotin

To better understand the charge heterogeneity of disitamab vedotin, SCX fractions of this ADC were collected, followed by native intact MS and peptide mapping, respectively. As Figure S5A showed, four fractions: acidic peaks (AP), main peak 1 (M1), main peak 2 (M2) and basic peaks (BP), were collected separately. Fig. 5 displayed the native intact raw spectra and deconvolution results of disitamab vedotin and each fraction, and obvious differences can be observed from peak to peak. Similar to online SCX-UV-MS, the drug payload increased along with the pI. The peptide mapping results of each fraction provided more details of the conjugation isomers with the same number of payloads. As displayed in Figure S5B, the relative abundance of the hinge region peptide *THTC(224)PPC(227)PAPELLGGPSVFLFPPKPK* isomers varied among the different fractions, indicating differences in conjugation site. In AP and M1, the relative abundance of *THTC(224+MC-vc-PAB-MMAE)PPC(227+carboxymethylation)PAPELLGGPSVFLFPPKPK* was greater than that of *THTC(224+carboxymethylation)PPC(227+MC-vc-PAB-MMAE)PAPELLGGPSVFLFPPKPK*, but the opposite was true for M2 and BP. The abundances of C224 and C227 both conjugated hinge region peptides were quite different in each fraction. In M2 and BP, the abundance of this peptide was much greater than that in AP and M1. Figure S5C displays the relative abundance of hinge region peptides with different modifications in each fraction. The conjugation% increased with increasing pI, which was in agreement with the MS results obtained for SCX-UV-MS and native intact MS of fractions.

The conjugation% of *GEC(212)* and *SC(218)DK* were greater than 96%, which indicated that LC–HC interchain disulphide was easier to be reduced for conjugation compared to hinge region interchain disulphides. Table 1 listed the details of the conjugation isomers in each fraction. In peak M1, two D4 isomers were identified. The percentage of the (LC–HC disulphide bonds)\*2 conjugated isomer was greater than that of the hinge region disulphide bonds\*2 conjugated isomer. In contrast, in peak M2, the (LC–HC disulphide bonds)\*2 conjugated, LC–HC + hinge region conjugated and hinge region disulphide bonds\*2 conjugated isomers were all identified, and the abundances of these three isomers decreased in that order. Two isomers of D6 were identified

in peak BP. The LC–HC disulphide bond-conjugated D2 isomer was the most abundant among all D2 isomers from all peaks. Other PTMs, such as deamidation, succinimidation, oxidation and lysine truncation of the heavy chain C-terminal, were illustrated in Figure SSD in the Supporting Information 7. The percentage of lysine truncation of the heavy chain C-terminal in BP was lower than that in the other fractions, as expected; the relative abundance of other PTMs also varied among the different fractions. Characterization of SCX fractions, both intact and peptide mapping level, helps to understand conjugation site-induced charge heterogeneity better; for example, isomers carrying the same payload can be eluted and detected in different SCX peaks because payloads are conjugated to different cysteines.

### 3.5. icIEF-MS under near-native condition for charge heterogeneity characterization of disitamab vedotin

icIEF-MS online coupling under denaturing condition is currently a mature workflow and has been used in mAb and fusion protein charge variant analysis [24,30,36,37]. However, icIEF-MS online coupling under native condition is quite challenging because the MS signal intensity of proteins is much lower under native condition as compared to denaturing condition, so the sensitivity of native MS is critical, especially for identifying low abundance charge variants. In addition, the make-up liquid needs to be changed to MS-compatible buffer while keeping the samples native. For the native cysteine-linked ADC analysis, the combination of make-up liquid (10 mM NH<sub>4</sub>Ac:ACN=9:1) and mobilization liquid (0.1% formic acid, H<sub>2</sub>O) can maintain the molecule under native state. However, when preparing ADC sample for icIEF analysis, a common approach is to add formamide to the sample solution to improve the solubility and decrease protein aggregation. However, formamide is a denaturing reagent and breaks the non-covalent bonds between the chains of cysteine-linked ADCs (data not shown). To keep the ADC sample at its native state, we chose the absence of formamide in the ADC sample as the final condition. As shown in the icIEF-UV and icIEF-MS profiles in Fig. 6A, four acidic peaks, one main peak and two basic peaks were separated and identified. Without formamide in the sample, the separation resolution decreased at icIEF level (Fig. 6A), but the HRMS platform used in this study could provide ultra-high

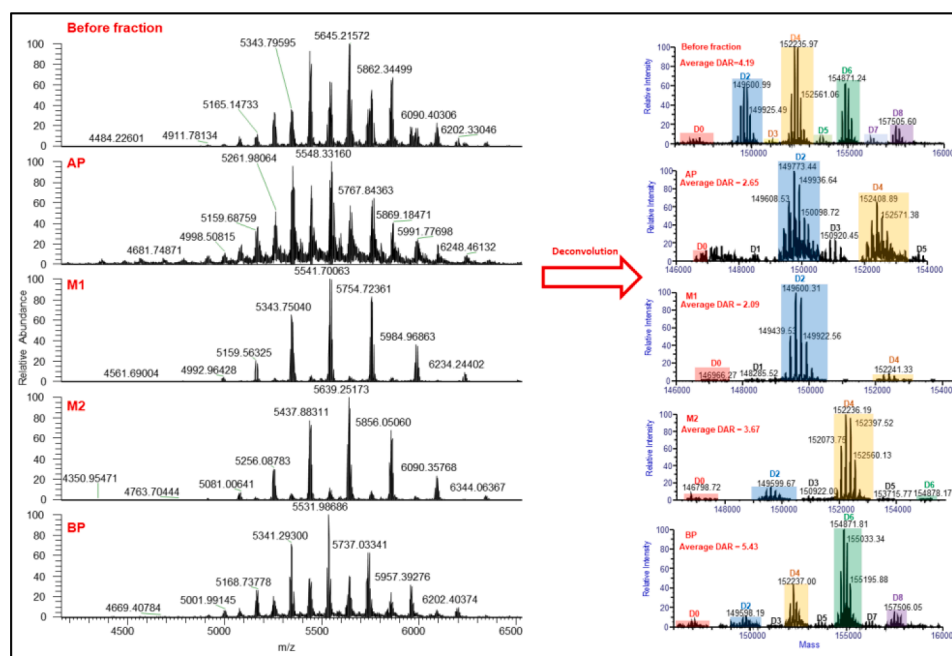


















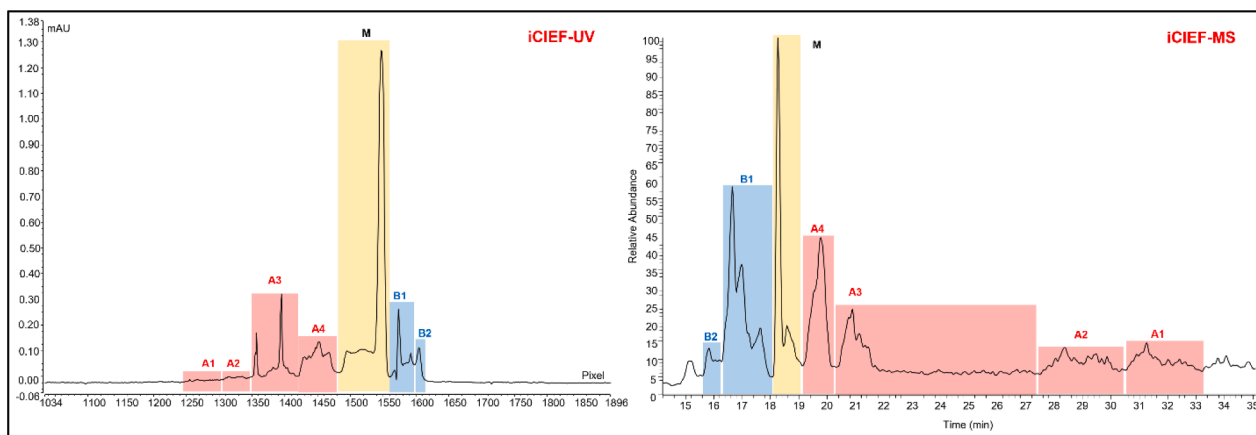


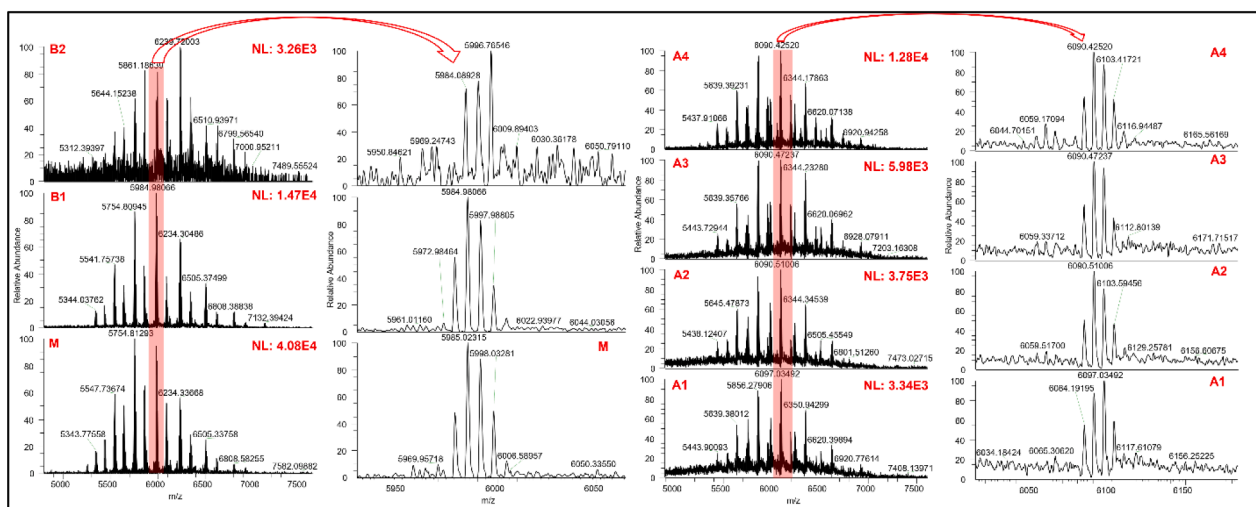
Fig. 5. Native intact results of disitamab vedotin offline SCX fractions. Left, raw spectra of intact ADCs. Right, the deconvolution results of the SCX fractions. The top row shows disitamab vedotin before fractionation, which was used as a reference.

**Table 1**  
Details of the conjugation isomers in each SCX fraction.

AP	M1	M2		BP	
 <b>D0</b> Carboxymethylation	 <b>D2</b> GEC - MMAE SCDK - MMAE Hinge region Carboxymethylation*2	 <b>D2</b> GEC - MMAE or Carboxymethylation SCDK - MMAE or Carboxymethylation Hinge region Carboxymethylation*2	 <b>D4</b> GEC - MMAE SCDK - MMAE Hinge region Carboxymethylation*2	 <b>D4</b> GEC - MMAE SCDK - MMAE Hinge region - Carboxymethylation*2	 <b>D6</b> GEC - MMAE or Carboxymethylation SCDK - MMAE or Carboxymethylation Hinge region - MMAE*2
 <b>D2</b> GEC - MMAE SCDK - MMAE Hinge region Carboxymethylation*2	 <b>D4</b> GEC - MMAE SCDK - MMAE Hinge region Carboxymethylation*2	 <b>D2</b> GEC Carboxymethylation SCDK Carboxymethylation Hinge region MMAE+Carboxymethylation	 <b>D4</b> GEC - MMAE or Carboxymethylation SCDK - MMAE Carboxymethylation Hinge region MMAE Carboxymethylation	 <b>D4</b> GEC - MMAE or Carboxymethylation SCDK - MMAE or Carboxymethylation Hinge region MMAE Carboxymethylation	 <b>D6</b> GEC - MMAE SCDK - MMAE Hinge region MMAE Carboxymethylation
 <b>D4</b> GEC - MMAE SCDK - MMAE Hinge region MMAE+Carboxymethylation	 <b>D4</b> GEC Carboxymethylation SCDK Carboxymethylation Hinge region - MMAE*2		 <b>D4</b> GEC Carboxymethylation SCDK Carboxymethylation Hinge region - MMAE*2	 <b>D4</b> GEC Carboxymethylation SCDK Carboxymethylation Hinge region - MMAE*2	 <b>D8</b> GEC - MMAE SCDK - MMAE Hinge region MMAE*2
				 <b>D2</b> GEC - MMAE or Carboxymethylation SCDK - MMAE or Carboxymethylation Hinge region - Carboxymethylation*2	



(A)



(B)

**Fig. 6.** Charge variant analysis of disitamab vedotin (3.2  $\mu$ g sample was loaded) using online coupling icIEF-MS under near-native condition. (A), icIEF-UV (left) and icIEF-MS (right) profiles. (B), Raw spectra of all peaks. (C), Deconvoluted spectra of all peaks. Red dotted box, deconvoluted spectra of basic peak1 (B1) and expanded view of D2 and D4 in B1.

resolution to compensate for this loss without the addition of formamide. Another advantage of the HRMS platform is its excellent sensitivity. In this experiment, only 3.2  $\mu$ g ADC sample was loaded, which is quite low for intact MS analysis under native condition. Even for the low abundance acidic peak 1 (with a relative abundance of 0.88 %), the S/N of the raw spectra was high, as shown in Fig. 6B.

D2 and D4 carrying one lysine at the C-terminal of the heavy chain were identified in basic peak 2 (B2), as shown in Fig. 6C. Basic peak 1 (B1) was a mixture of D0 to D6 with  $2 \times K$  loss, and D2 was the most abundant payload isoform. The N-glycosylation distributions of D2 and D4 were shown in the expanded view of Fig. 6C, and the low abundance N-glycoform A2G0F+A2G0 was detected. The major components in the main peak were D2 and D4 N-glycosylation distributions with  $2 \times K$  loss. The relative abundance of D4 was greater in the main peak than that of B2 (Fig. 6C). Among the acidic peaks, the most abundant payload isoform was D4, and D8 was detected in acidic peaks 4 and 3 (A4 and A3), as shown in Fig. 6C. Deamidation variants were observed in the acidic peaks, as expected. Minor odd-number payload isoforms, such as D3, D5 and D7, were detected in agreement with the native intact MS results. In this study, it was speculated that icIEF separates charge variants of cysteine-linked ADC based on PTM-induced charge heterogeneity more

than conjugation-induced heterogeneity.

### 3.6. The prospect of integrating traditional chromatography and electromigration for the MS characterization of extremely complex therapeutic biopharmaceuticals

Due to different separation mechanisms, there is a divergence between icIEF-MS and IEX-MS when diverse protein samples are analyzed, especially for extremely complex therapeutic biopharmaceuticals. Hence, integrating icIEF-MS and IEX-MS contributes to a more in-depth characterization of protein charge variants. Wu et al. compared the performances of developed icIEF-MS and SCX-MS in terms of throughput, sensitivity, repeatability and accuracy when both MS online tools were applied to the characterization of nine therapeutic mAb charge variants [24]. Xing et al. compared IEX and icIEF as front-end separation techniques for mass spectrometry-based charge variant analysis of therapeutic bispecific antibody[46]. Native SCX-MS could provide in-depth charge variant information for each fraction collected by preparative icIEF with a limited sample amount. Recently, Prof. Karger, in his review on capillary electrophoresis in Trends in Analytical Chemistry [47], highlighted that "Isoelectric focusing, as we have noted,



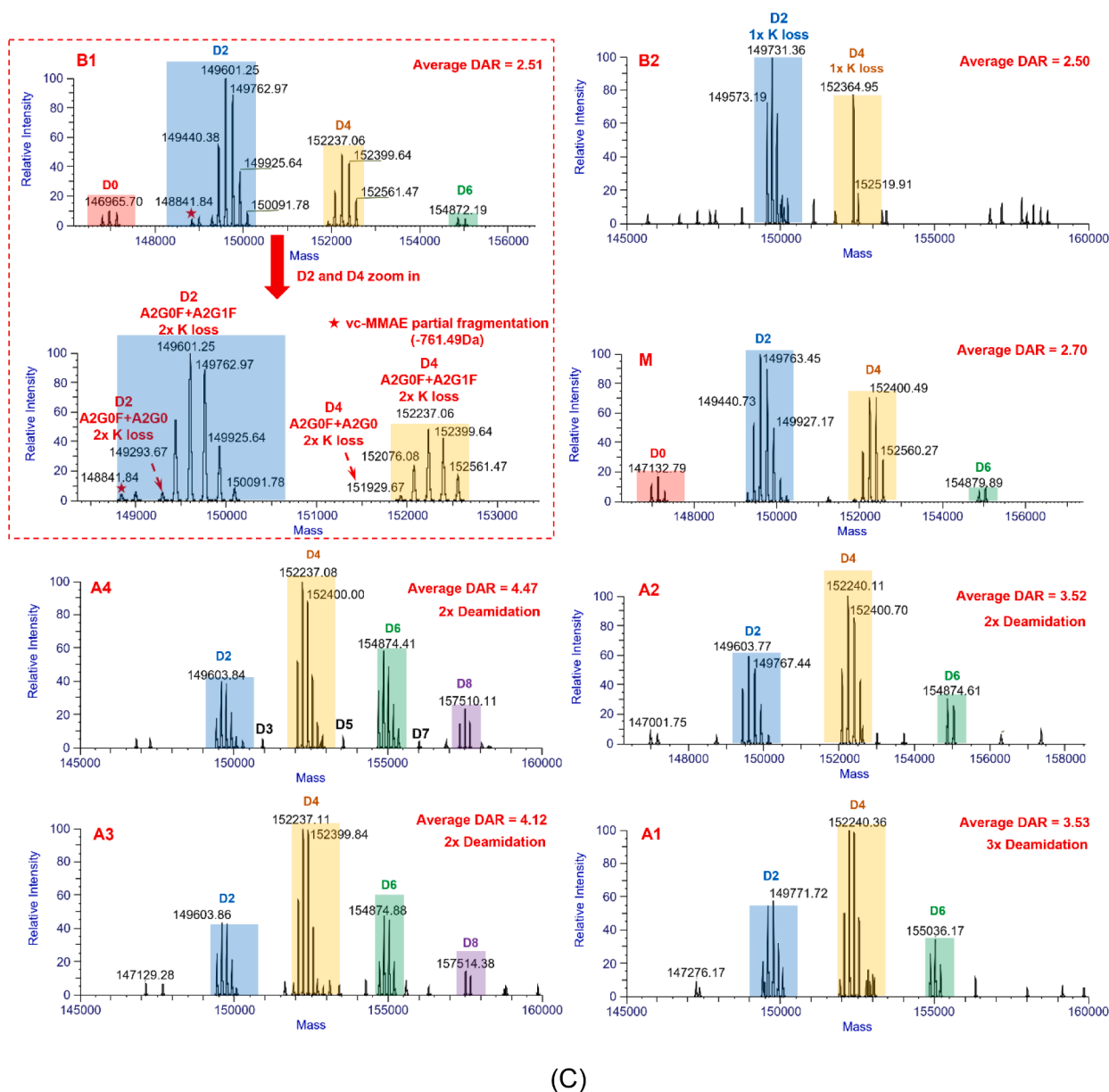


Fig. 6. (continued).

is an important protein characterization method and is widely used in CE. However, the coupling of CE and MS has been limited in part because of interference by the carrier ampholytes. There is a clear need for on-line coupling of cIEF and MS as isolation of specific cIEF peaks for MS analysis can take days to complete. There is active work going on direct cIEF-MS coupling and even MS coupling to imaged cIEF, generally using low levels of ampholytes. We can anticipate increasing use of cIEF-MS systems." A combination of traditional chromatography and electromigration methods for the MS characterization of extremely complex therapeutic biopharmaceuticals can enable more in-depth and more accurate characterization of complex charge heterogeneities.

#### 4. Conclusions

Due to the complexity of cysteine-linked ADCs, a workflow involving comprehensive separation techniques coupled with high-resolution MS was developed for dissecting complex heterogeneity. Traditional UHPLC-MS and UHPLC-MSMS were utilized for characterizing disitamab vedotin via native intact protein analysis, reduced chains and

subunit analysis under denaturing condition, and peptide mapping with PTM identification. Using this integrated MS-based workflow, disitamab vedotin was successfully characterized, and the CQAs of the ADC, including the DAR, DLD and conjugation sites, were assessed.

Considering that payload conjugation can increase the charge heterogeneity of ADC molecules, multiple charge heterogeneity separation techniques, including SCX-UV-MS, SCX fractionation integrating native intact MS and peptide mapping, and icIEF-MS under near-native condition were explored to investigate their ability to separate ADC charge variants, performed real-time MW measurements and characterize the resulting fractions. SCX and icIEF are widely used for biotherapeutics characterization, but not so much reports on direct coupling to MS. The high resolution MS platform can provide more comprehensive information of ADC charge variants, such as molecular weight and PTMs. The combination of comprehensive techniques has provided rich information on ADC charge variants, which came from the charge heterogeneity of mAbs and payload conjugation. Moreover, the integration of SCX-MS and icIEF-MS under near-native condition provided a fast overview of ADC charge variant screening information at intact level. Due to

differences in separation mechanisms, SCX-UV-MS can separate ADCs based on payload conjugation-induced heterogeneity more than on PTM-induced charge heterogeneity, while icIEF-MS has the opposite effect, so the two assays could provide complementary results. Also, the make-up solution flow rate for icIEF-MS is lower than SCX-UV-MS, which helps to improve the sensitivity. This can be critical because we need to identify low abundant variants and the MS signal of proteins are usually one to two orders lower under native condition compares to denaturing condition. The characterization of the SCX fractions included more details on the SCX-UV-MS results, for example, the distribution of conjugation site isomers in each fraction.

For the first time, our study introduced cutting-edge icIEF-MS under near-native condition for in-depth characterization of cysteine-linked ADC disitamab vedotin, which was integrated with traditional online chromatography-MS approaches. Although CE based separation techniques online coupling with MS were already applied in protein charge variant analysis, these approaches have limitations for cysteine-linked ADC analysis. For example, icIEF-MS under denaturing condition will break the non-covalent bindings between light chains and heavy chains; microfluidic chip based CE/CZE-MS[23] has the challenge in method bridging and transfer from development to QC; Sun et al. [38]. published cIEF-MS under native condition was a good attempt, but better data quality could be obtained with higher mass spectral resolution and sensitivity. Therefore, icIEF-MS under near-native condition we developed in this work can keep the cysteine-linked ADC stay native during the icIEF separation and MS detection, also enables easily seamless icIEF method transfer from development to QC. This workflow underlined the outstanding importance of comprehensive separation techniques based on MS technology in the development of ADCs.

#### CRediT authorship contribution statement

**Gang Wu:** Writing – review & editing, Methodology, Conceptualization. **Xiaoxi Zhang:** Writing – original draft, Investigation. **Xin Wang:** Validation. **Jialiang Du:** Validation. **Meng Li:** Funding acquisition. **Gangling Xu:** Funding acquisition. **Min Du:** Formal analysis. **Chuanfei Yu:** Supervision.

#### Declaration of competing interest

The authors have declared no conflict of interest.

#### Data availability

Data will be made available on request.

#### Acknowledgements

This work was supported by the Research on precise quantitative technology of protein biological products under the National Key Research and Development Program of China (No. 2023YFC3404004) and Project of State Key Laboratory of Drug Regulatory science (No. 2023SKLDRS0118).

The authors gratefully acknowledge Dr. Tao Bo from Advanced Electrophoresis Solutions Ltd. (AES) for providing technical support for this work.

#### Supplementary materials

Supplementary material associated with this article can be found, in the online version, at [doi:10.1016/j.chroma.2024.465353](https://doi.org/10.1016/j.chroma.2024.465353).

#### References

- [1] C. Dumontet, et al., Antibody-drug conjugates come of age in oncology, *Nat. Rev. Drug Discovery* 22 (2023) 641–661.
- [2] P.F. Bross, J. Beitz, G. Chen, X.H. Chen, E. Duffy, L. Kieffer, et al., Approval summary: gemtuzumab ozogamicin in relapsed acute myeloid leukemia, *Clin. Cancer Res.* 7 (6) (2001) 1490–1496.
- [3] A. Beck, T. Wurch, C. Bailly, N. Corvaia, Strategies and challenges for the next generation of therapeutic antibodies, *Nat. Rev. Immunol.* 10 (5) (2010) 345–352.
- [4] Seattle Genetics' Antibody-Drug Conjugate Receives FDA Okay to Treat Lymphomas, *Genetic Engineering & Biotechnology News* (2011). <https://www.genengnews.com/topics/drug-discovery/seattle-genetics-antibody-drug-conjugate-receives-fda-okay-to-treat-lymphomas/>, 22 August.
- [5] "FDA approves new treatment for late-stage breast cancer" (Press release). U.S. Food and Drug Administration (FDA). <https://www.fda.gov/NewsEvents/Newsroom/PressAnnouncements/ucm340704.htm> 22 February 2013.
- [6] J.A. Francisco, et al., cAC10-vcMMAE, an anti-CD30-monomethyl auristatin E conjugate with potent and selective antitumor activity, *Blood* 102 (4) (2003) 1458–1465.
- [7] S. Verma, D. Miles, L. Gianni, et al., Trastuzumab emtansine for HER2-positive advanced breast cancer, *N. Engl. J. Med.* 367 (19) (2012) 1783–1791.
- [8] "Kadcyla- ado-trastuzumab emtansine injection, powder, lyophilized, for solution". <https://dailymed.nlm.nih.gov/dailymed/drugInfo.cfm?setid=23f3c1f4-0fc8-4804-a9e3-04cf25dd302e> DailyMed. 16 May 2019. Retrieved 4 December 2019.
- [9] "Adcetris- brentuximab vedotin injection, powder, lyophilized, for solution". <https://dailymed.nlm.nih.gov/dailymed/drugInfo.cfm?setid=3904f8dd-1aef-3490-e48f-bd55f32ed67f> DailyMed. 26 November 2018. Retrieved 19 August 2020.
- [10] "FDA Drug Safety Communication: New Boxed Warning and Contraindication for Adcetris (Brentuximab vedotin)", U.S. Food and Drug Administration (FDA), 2012. <https://www.fda.gov/drugs/drug-safety-and-availability/fda-drug-safety-communication-new-boxed-warning-and-contraindication-adcetris-brentuximab-vedotin>. Retrieved 19 August 2020.
- [11] Z. Fu, S. Li, S. Han, et al., Antibody drug conjugate: the "biological missile" for targeted cancer therapy, *Sig Transduct Target Ther* 7 (2022) 93.
- [12] E.D. Deeks, Disitamab Vedotin: first Approval, *Drugs* 81 (2021) 1929–1935.
- [13] F. Shi, Y. Liu, X. Zhou, P. Shen, R. Xue, M. Zhang, Disitamab vedotin: a novel antibody-drug conjugates for cancer therapy, *Drug Deliv.* 29 (1) (2022) 1335–1344, <https://doi.org/10.1080/10717544.2022.2069883>.
- [14] E. Bourbon, G. Salles, Polatumab vedotin: an investigational anti-CD79b antibody drug conjugate for the treatment of diffuse large B-cell lymphoma, *Expert Opin. Investig. Drugs* 29 (10) (2020) 1079–1088.
- [15] Y. Jin, Z. Lin, Q. Xu, C. Fu, Z. Zhang, Q. Zhang, W.A. Pritts, Y. Ge, Comprehensive characterization of monoclonal antibody by Fourier transform ion cyclotron resonance mass spectrometry, *MAbs* 11 (1) (2019) 106–115.
- [16] F. Higel, A. Seidl, F. Sörgel, W. Friess, N-glycosylation heterogeneity and the influence on structure, function and pharmacokinetics of monoclonal antibodies and Fc fusion proteins, *Eur. J. Pharm. Biopharm.* 100 (2016) 94–100.
- [17] L.D. Bastiaan, A. Murisier, J. Camperi, S. Fekete, A. Beck, D. Guillaume, V D'Atri, Therapeutic Fc-fusion proteins: current analytical strategies, *J. Sep. Sci.* 1 (2020) 35–62.
- [18] Y.T. Yan, T. Xing, S.H. Wang, N Li, Versatile, sensitive, and robust native LC-MS platform for intact mass analysis of protein drugs, *J. Am. Soc. Mass Spectrom.* 31 (2020) 2171–2179.
- [19] S. Tamara, M.A. den Boer, A.J.R. Heck, High-Resolution Native Mass Spectrometry, *Chemical Review* 122 (8) (2022) 7269–7326.
- [20] B.L. Duivelshof, A. Beck, D. Guillaume, V D'Atri, Bispecific antibody characterization by a combination of intact and site-specific/chain-specific LC/MS techniques, *Talanta* 236 (2022) 122836.
- [21] S. Chapel, F. Rouvière, M. Sarrut, S. Heinisch, Two-dimensional liquid chromatography coupled to high-resolution mass spectrometry for the analysis of ADCs, *Methods Mol. Biol.* 2078 (2020) 163–185.
- [22] H. Kaur, J. Beckman, Y.T. Zhang, Z.J. Li, M. Szigeti, A Guttman, Capillary electrophoresis and the biopharmaceutical industry: therapeutic protein analysis and characterization, *Trends Anal. Chem.* 144 (2021) 116407.
- [23] F. Füssli, A. Trappe, S. Carrillo, C. Jakes, J. Bones, Comparative elucidation of cetuximab heterogeneity on the intact protein level by cation exchange chromatography and capillary electrophoresis coupled to mass spectrometry, *Anal. Chem.* 92 (7) (2020) 5431–5438.
- [24] G. Wu, C.F. Yu, W.B. Wang, L.J. Du, Z.H. Fu, G.L. Xu, M. Li, L. Wang, Mass spectrometry-based charge heterogeneity characterization of therapeutic mAbs with imaged capillary isoelectric focusing and ion-exchange chromatography as separation techniques, *Anal. Chem.* 95 (2023) 2548–2560.
- [25] J.Q. Wu, W. McElroy, J. Pawliszyn, C.D. Heger, Imaged capillary isoelectric focusing: applications in the pharmaceutical industry and recent innovations of the technology, *Trends Anal. Chem.* 150 (2022) 116567.
- [26] J. Lin, A.C. Lazar, Determination of charge heterogeneity and level of unconjugated antibody by imaged cIEF, *Methods Mol. Biol.* 1045 (2013) 295–302.
- [27] L.A. Khowli, S. Goswami, R. Hutchinson, Z.W. Kwong, J. Yang, X. Wang, Z. Yao, A. Sreedhara, T. Cano, D. Tesar, et al., Charge variants in IgG1: isolation, characterization, in vitro binding properties and MABS 241 pharmacokinetics in rats, *MAbs* 2 (2010) 613–624.
- [28] X. Zhang, L. Chemmalil, J. Ding, N. Mussa, Z. Li, Imaged capillary isoelectric focusing in native condition: a novel and successful example, *Anal. Biochem.* 537 (2017) 13–19.
- [29] X.X. Zhang, T. Kwok, M. Zhou, M. Du, T. Chen, V. Li, T. Bo, T.M. Huang, Imaged capillary isoelectric focusing (icIEF) tandem high resolution mass spectrometry for

- charged heterogeneity of protein drugs in biopharmaceutical discovery, *J. Pharm. Biomed. Anal.* 224 (2023) 115178–115189.
- [30] J. Schlecht, B. Moritz, S. Kiessig, C. Neustüß, Characterization of therapeutic mAb charge heterogeneity by icIEF coupled to mass spectrometry (icIEF-MS), *Electrophoresis* 44 (5–6) (2023) 540–548.
- [31] T. Kwok, S.L. Chan, M. Courtney, M. Zhou, T.M. Huang, T. Bo, V. Li, T. Chen, Imaged capillary isoelectric focusing tandem high-resolution mass spectrometry using nano electrospray ionization (ESI) for protein heterogeneity characterization, *Anal. Biochem.* 680 (2023) 115312.
- [32] X.P. He, M. ElNaggar, M.A. Ostrowski, A. Guttman, E. Gentalen, J. Sperry, Evaluation of an icIEF-MS system for comparable charge variant analysis of biotherapeutics with rapid peak identification by mass spectrometry, *Electrophoresis* 43 (2022) 1215–1222.
- [33] M.A. Ostrowski, S. Mack, M. Ninonuevo, J. Yan, M. ElNaggar, E. Gentalen, Rapid multi-attribute characterization of intact bispecific antibodies by a microfluidic chip-based integrated icIEF-MS technology, *Electrophoresis* 44 (2023) 378–386.
- [34] M. Scott, A. Don, B. Greg, B. Luc, D. Lieza, D. Vladislav, D. MaryAnn, G. Eric, H. Chris, J. Morten, J. Jennifer, L. Steve, R. Claudia, W. Ian, G. Erik, A novel microchip-based imaged CIEF-MS system for comprehensive characterization and identification of biopharmaceutical charge variants, *Electrophoresis* 40 (23–24) (2019) 3084–3091.
- [35] T. Kwok, M. Zhou, A. Schaefer, T. Bo, V. Li, T.M. Huang, T. Chen, Fractionation and online mass spectrometry based on imaged capillary isoelectric focusing (icIEF) for characterizing charge heterogeneity of therapeutic antibody, *Anal. Methods* 15 (2023) 411–418.
- [36] X.X. Zhang, T. Chen, V. Li, T. Bo, M. Du, T.M. Huang, Cutting-edge mass spectrometry strategy based on imaged capillary isoelectric focusing (icIEF) technology for characterizing charge heterogeneity of monoclonal antibody, *Anal. Biochem.* 660 (2023) 114961–114972.
- [37] G. Wu, J.L. Du, C.F. Yu, Z.H. Fu, X.X. Zhang, L. Wang, Z.J. Wang, Mass spectrometry study on SARS-CoV-2 recombinant vaccine with comprehensive separation techniques to characterize complex heterogeneity, *Analytical Chimica Acta* 1297 (2024) 342349.
- [38] T. Xu, L. Han, L. Sun, Automated capillary isoelectric focusing-mass spectrometry with ultrahigh resolution for characterizing microheterogeneity and isoelectric points of intact protein complexes, *Anal. Chem.* 94 (2022) 9674–9682.
- [39] J.F. Valliere-Douglass, W.A. McFee, O. Salas-Solano, Native intact mass determination of antibodies conjugated with monomethyl Auris-tatin E and F at interchain cysteine residues, *Anal. Chem.* 84 (2012) 2843.
- [40] V. D'Atri, S. Fekete, D. Stoll, M. Lauber, A. Beck, D. Guillaume, Characterization of an antibody-drug conjugate by hydrophilic interaction chromatography coupled to mass spectrometry, *J. Chromatogr. B* 1080 (2018) 37–41.
- [41] E.A. Redman, J.S. Mellors, J.A. Starkey, J.M. Ramsey, Characterization of intact antibody drug conjugate variants using microfluidic capillary electrophoresis-mass spectrometry, *Anal. Chem.* 88 (4) (2016) 2220–2226.
- [42] Y. Matsuda, M. Kliman, B.A. Mendelsohn, Application of native ion exchange mass spectrometry to intact and subunit analysis of site-specific antibody-drug conjugates produced by AJICAP first generation technology, *J. Am. Soc. Mass. Spectrom.* (2020).
- [43] E. Deslignière, H. Diemer, S. Erb, P. Coliat, X. Pivot, A. Detappe, O. Oscar Hernandez-Alba, S. Cianféroni, A combination of native LC-MS approaches for the comprehensive characterization of the antibody-drug conjugate trastuzumab deruxtecan, *Front. Biosci. (Landmark Ed)* 27 (10) (2022) 290.
- [44] M. Janin-Bussat, M. Dillenbourg, N. Corvaia, A. Beck, C. Klinguer-Hamour, Characterization of antibody drug conjugate positional isomers at cysteine residues by peptide mapping LC-MS analysis, *J. Chromatogr. B* 9–13 (2015) 981–982.
- [45] J.R. Junutula, H. Raab, S. Clark, S. Bhakta, D.D. Leipold, S. Weir, Y. Chen, M. Simpson, S.P. Tsai, M.S. Dennis, Y. Lu, Y.G. Meng, C. Ng, J. Yang, C.C. Lee, E. Duenas, J. Gorrell, V. Katta, A. Kim, K. McDorman, K. Flagella, R. Venook, S. Ross, S. D. Spencer, W. Lee Wong, H.B. Lowman, R. Vandlen, M.X. Sliwkowski, R. H. Scheller, P. Polakis, W. Mallet, Site-specific conjugation of a cytotoxic drug to an antibody improves the therapeutic index, *Nat. Biotechnol.* 26 (2008) 925.
- [46] T. Xing, Y.T. Yan, S.H. Wang, N. Li, Comparing Ion Exchange Chromatography and Capillary Isoelectric Focusing as Front-End Separation Techniques for Mass Spectrometry-Based Charge Variant Analysis of Therapeutic mAbs, Regeneron Inc., Poster, ASMS, 2022.
- [47] B.L. Karger, Perspectives on capillary electrophoresis, *Trends in Analytical Analysis* 167 (2023) 117215.